

# Improved Plasmonic Demultiplexer Based on Tapered and Rectangular Slot MIM Waveguide

Aso Rahimzadegan, Seyyed Poorya Hosseini, and Kamran Qaderi

**Abstract**—In this paper, we have proposed two novel plasmonic demultiplexing structures based on metal-insulator-metal surfaces which, beside their compact size, have a very good transmission spectrum. The impact of the key internal parameters on the transmission spectrum is numerically analyzed by using the two-dimensional (2D) finite difference time domain (FDTD) method. The proposed structures could be used to develop ultra-compact photonic wavelength demultiplexing devices for large-scale photonic integration.

**Keywords**—Photonic integrated devices, Plasmonics, Metal-insulator-metal (MIM) waveguide, Demultiplexers.

## I. INTRODUCTION

MODERN electronic devices are rapidly approaching their fundamental speed and bandwidth limitations, which is a serious impediment for new applications and requirements. Carrying information by light and replacing electronic signals by lightwave is an auspicious solution towards higher speeds. The diffraction limit did not allow the localization of light in areas smaller than the wavelength; therefore, miniaturization and integration of photonic circuits were impossible [1]. Excitation of surface plasmons is one of the most feasible ways to guide electromagnetic waves beyond diffraction limit in order to control light in the nanometer scales. Estimations show that data rates of 10Tbit/s are achievable by decreasing the photonic devices to subwavelength scales [2].

Different metallic plasmonic nanoguiding structures have been proposed. These include thin metal films, metal nanorods, metal wedges, nanogrooves, slot waveguides, etc. Different aspects and properties of these devices are studied in [1]. Two of the well-known multilayer waveguides are metal-insulator-metal (MIM) and insulator-metal-insulator (IMI) structures. MIM structure gives more light confinement, but more propagation loss (less propagation length), whereas IMI structure is vice versa. Therefore, there should be a tradeoff between propagation length and confinement. It is shown that MIM structure is a superior choice [3]. It is experimentally verified that silver, due to its lower guiding loss, is the proper metal for plasmonic waveguides [4].

A. Rahimzadegan is with the Young Researchers and Elite club, Boukan Branch, Islamic Azad University, Boukan, Iran (phone: +98-919-507-6554; e-mail: aso.rahimzadegan@gmail.com).

S. P. Hosseini is with the electrical engineering department, K. N. Toosi University of Technology (poorya\_hosseini@ee.kntu.ir).

K. Qaderi is with the Electrical Engineering Department, Iran University of Science and Technology (IUST), Tehran, Iran, (e-mail: kamran\_qaderi@elec.iust.ac.ir).

To realize photonic circuitry based on plasmonics, a variety of components are required: splitters [5]-[7], couplers [8]-[9], multiplexers and demultiplexers [10]-[13], switches [14], logic gates [15] etc., which have been studied recently.

Demultiplexers are key components of integrated circuitry. There are several plasmonic demultiplexer structures, which have been proposed. A plasmonic demultiplexer based on Y bent waveguide is presented in which there is a minimum space of  $2\mu\text{m}$  between the input and the output waveguides, which may not be desirable for compact circuitry [10]. Most demultiplexers lack a good transmission through their channels, which is mostly due to the weak coupling effect. In [12], a nanoplasmonic triple-wavelength demultiplexer is presented, but resonance frequencies are not transmitted properly and corresponding spectrum peak values are undesirably low. Tao, Huang and Zhu proposed a novel demultiplexer based on nano-capillary resonators with spectrum peak values of as low as -10dB in each channel, which is not a desirable transmission spectrum [16]. A novel multichannel wavelength demultiplexer based on slot cavities has been proposed, which can effectively omit the second mode and result in a single-band transmission, but like others, the channel transmission is accompanied by a significant loss of about -8dB in each channel [17].

In this paper, we have presented two novel ultra-compact demultiplexing structures which can efficiently demultiplex the desired wavelengths.

The paper is organized as follows; in Section II, some introductory concepts of plasmons and the FDTD method are discussed, and in Section III, the proposed structures and their numerical simulations are presented.

## II. SURFACE PLASMON POLARITONS AND THEIR ANALYSIS METHOD

Surface plasmon is a classic electromagnetic subject known since long years ago, but it has now become an intriguing field of research for scientists as a result of the recent advances in nanotechnology [18]. At optical frequencies, metals can be modeled by a gas of free electrons moving against a positive background ion cores known as plasma model. When located in an electromagnetic field, the electrons oscillate and their motion is damped with a characteristic collision frequency,  $\gamma$ . It has been assumed that the driving field is  $E(t) = E_0 \exp(-j\omega t)$  [19]. The permittivity function taken from this basic explication with some modification, called Drude-Lorentz model, is:

$$\varepsilon(\omega) = \varepsilon(\infty) - \frac{\omega_p^2}{\omega^2 + j\omega\gamma} + \sum_{i=1}^{i_{\max}} \frac{s_i \omega_i^2}{\omega_i^2 - \omega^2 - j\omega\gamma_i} \quad (1)$$

where  $\omega_p$  is the plasma angular frequency of the free electron gas,  $\omega$  is the angular frequency of the lightwave,  $\varepsilon(\infty)$  is the high-frequency (electronic transition) contribution to the dielectric constant,  $\omega_i$  denotes the oscillation frequency of the  $i$ th bound electron under an applied electric potential, and  $s_i$  and  $\gamma_i$  are related to the density and damping of those bound electrons, respectively [20]-[21].

In this paper, we have used the silver parameters of:  $\varepsilon(\infty) = 3.7$ ,  $\omega_p = 1.38 \times 10^{16} \text{ rad/s}$  and  $\gamma = 0.27 \times 10^{14} \text{ rad/s}$  [10], [12], [22]. Other parameters are given in Table I.

TABLE I  
 PARAMETERS OF THE DRUDE-LORENTZ MODEL FOR SILVER [23].

i	$\omega_i$ (eV)	$\gamma_i$ (eV)	$s_i$
1	0.816	3.886	0.065
2	4.481	0.452	0.124
3	8.185	0.065	0.011
4	9.083	0.916	0.840
5	20.29	2.419	5.646

A plasmon is a quasiparticle and quantum of plasma oscillation of free electrons. Plasmons with collective electron oscillations confined to an interface of a metal and a dielectric are called surface plasmons (SPs). When a photon (a quantum of electromagnetic wave) is coupled to an SP, another quasiparticle called surface plasmon polariton (SPP) is produced. SPPs are surface electromagnetic waves propagating along the interface of a metal-dielectric and evanescently confined in the perpendicular direction [2]. This coupling helps the lightwave to be transmitted at the interface of a metal-dielectric and consequently the diffraction limit would not be a problem for subwavelength light guiding anymore.

Solving Helmholtz equation and applying boundary conditions show that SPPs exist only for TM modes. This is due to the negative real part of the dielectric function of metal at optical frequencies [19]. However, lightwave cannot directly excite SPPs in normal conditions, because the photons' momentum is lower than that of the SPP. Coupling techniques are required to compensate the momentum. Prism coupling, scattering from a topological defect such as subwavelength protrusion or hole, and using periodic corrugations in the metal's surface are the main coupling techniques. Once light is coupled to SPPs, it will be propagated along the interface and will also be attenuated accordingly [18].

To simulate the plasmonic filters, we have used the FDTD method in which Maxwell's equations are solved by discretizing time and space. The spatial grid size is  $\Delta z = \Delta x = 4 \text{ nm}$ , which was found to be sufficient for numerical convergence. Our two-dimensional simulation box uses convolutional perfectly matched layer (CPML) in the boundaries in order to virtually simulate an infinite space for

the propagating wave and prevent reflections of outgoing waves. Due to the Courant condition, the time integration step is  $\Delta t = (0.6 \Delta x / c) \text{ s}$ .

The numerical calculations are convergent for the number of time steps of up to  $2^{20}$ . Simulation of large number of cells and time steps is a lengthy procedure and needs a lot of considerations in the process of code writing to conserve time as much as possible. For example, if the codes are written in MATLAB, "for" loops should be swapped with matrix calculations. A very important point to be noticed is the distance of the source from CPML layers, which should be far enough to converge the numerical simulations. The space of  $1 \mu\text{m}$  was required in order to avoid instability of the numerical simulations.

### III. ANALYSIS AND SIMULATIONS

#### A. Tapered Demultiplexer

A novel demultiplexer system is presented in Fig. 1 (a). The input waveguide is interlinked to two demultiplexing channels through two cavities with lengths of  $L_1$  and  $L_2$ . The incident wave is either reflected from or coupled to the cavities. Constructive reflections inside the cavities at a specific wavelength, form standing waves and the structure operates as a resonance device. Therefore, the incident wave is passed or blocked and each cavity operates as a narrow band-pass filter. Resonance wavelength is linearly related to the length of the cavity. So using different lengths for the two cavities can build a two-channel demultiplexer. The cavities lengths are adjusted so that the resonance wavelengths are 1319nm and 1545nm. Design parameters are given in the figure caption. Magnetic field distributions for two wavelengths are also demonstrated in Figs. 1 (c) and 1 (d) to show the demultiplexing performance of the device. The impacts of slope of the input taper,  $S_i$ , on the quality factor and spectrum peak value is shown in Fig. 1 (e). Quality factor is one of the most important characteristics of filters defined as  $Q = \lambda_r / \Delta\lambda$ , where  $\lambda_r$  is the resonance wavelength of the cavity and  $\Delta\lambda$  is the full width at half maximum (FWHM) of transmission spectrum. Simulations show that steeper slopes result in better transmission with lower loss, but simultaneously decrease the quality factor of the transmission spectrum. Also, it would make the fabrication more difficult, so there should be a tradeoff. Numerical results are given in table II. Without considering footprints of the input and output waveguides, the demultiplexer length is as small as 900nm, which is a compact structure compared to other conventional demultiplexers, which is very desirable for integrated photonic circuitry.

The structure can be designed for triple-wavelength demultiplexing. Owing to the flexibility for variation of the cavities' lengths, other desired distant enough demultiplexing frequencies with more channels are achievable.

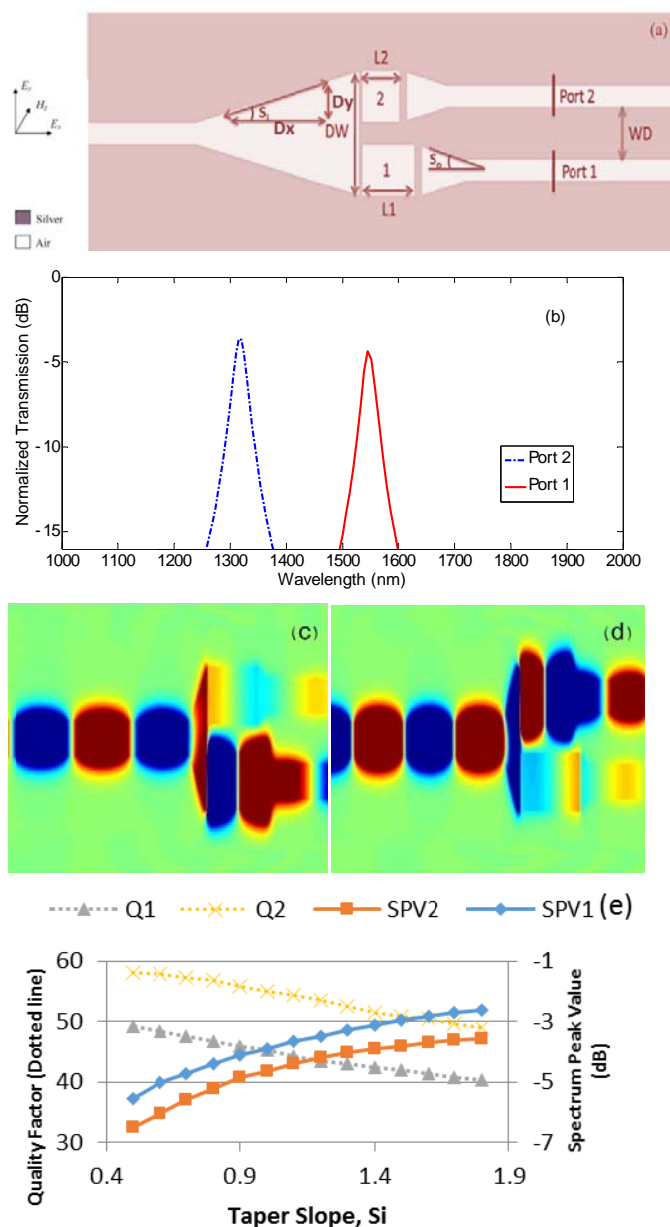


Fig. 1 (a) Schematic view of the proposed demultiplexer structure (b) Its transmission spectra with cavity lengths of  $L_1=628\text{nm}$ ,  $L_2=524\text{nm}$ , cavity widths of  $W_1=W_2=164\text{nm}$ , waveguide width,  $d=100\text{nm}$ , metallic gap size,  $G=16\text{nm}$ ,  $DW=416\text{nm}$ ,  $S_i=0.9$ ,  $S_o=0.5$ . Magnetic field distributions for wavelengths of (c)  $1319\text{nm}$ , demonstrating the demultiplexing performance of the proposed device (e) Quality factor and spectrum peak value (SPV) of both channels, versus input taper slope,  $S_i$ , assuming waveguide width,  $d=100\text{nm}$ ,  $L_1=628\text{nm}$ ,  $L_2=524\text{nm}$ , cavity widths of  $W_1=W_2=164\text{nm}$ , metallic gap size,  $G=16\text{nm}$ ,  $DW=416\text{nm}$ ,  $S_o=0.5$

TABLE II  
SIMULATED SPECIFICATIONS OF THE TAPERED DEMULTIPLEXER WITH WAVEGUIDE WIDTH,  $d=100\text{nm}$ ,  $L_1=628\text{nm}$ ,  $L_2=524\text{nm}$ , CAVITY WIDTHS OF  $W_1=W_2=164\text{nm}$ , METALLIC GAP SIZE,  $G=16\text{nm}$ ,  $DW=416\text{nm}$ ,  $S_o=0.5$

$S_i$	$Q_1, Q_2$	$SPV_1(\text{dB}), SPV_2(\text{dB})$	$\lambda_1(\text{nm}), \lambda_2(\text{nm})$
0.5	49,58	-5.6,-6.5	1319,1545
0.6	48,58	-5.0,-6.0	1319,1545
0.7	48,57	-4.7,-5.6	1319,1545
0.8	47,57	-4.4,-5.2	1319,1545
0.9	46,56	-4.1,-4.9	1319,1545
1.0	45,55	-3.9,-4.6	1319,1545
1.1	44,54	-3.7,-4.4	1314,1545
1.2	43,53	-3.5,-4.2	1314,1551
1.3	43,53	-3.3,-4.0	1324,1551
1.4	42,52	-3.1,-3.9	1329,1551
1.5	42,51	-3.0,-3.8	1349,1558
1.6	41,50	-2.8,-3.7	1319,1545
1.7	41,50	-2.7,-3.6	1319,1545
1.8	40,49	-2.6,-3.6	1319,1545

### B. Rectangular Demultiplexer

Another demultiplexer structure has been studied. The structure is shown in Fig. 2. This time, instead of a tapered input waveguide, a rectangular slot with a length of  $L_3$  is added to the structure. The cavities lengths are adjusted so that the resonance wavelengths are  $1329\text{nm}$  and  $1551\text{nm}$ . Design parameters are given in the figure caption. Magnetic field distributions for two wavelengths are also demonstrated in Figs. 2 (c) and 2 (d) to show the demultiplexing performance of the device. The impacts of rectangular slot length,  $L_3$ , on the quality factor and spectrum peak value are shown in Fig. 2 (e). Numerical results are given in Table III. The shorter rectangular slot results in better transmission with lower loss, but decreases the quality factor.

The structure can be designed for triple-wavelength demultiplexing. Owing to the flexibility for variation of the cavities' lengths, other desired distant enough demultiplexing frequencies with more channels are achievable.

A comparison of the two structures shows a better performance of the tapered demultiplexer in some cases and rectangular demultiplexer in other cases depending on the resonance wavelength. By better performance we mean that with a constant spectrum peak value, a better quality factor is achieved. Therefore, for any design, the numerical results in tables II and III should be considered.

In summary, we have proposed two novel demultiplexing structures which, beside their compact size, have a very good transmission spectrum. Our results imply potential applications of the proposed structures in the nanoscale integrated photonic circuits on the flat metallic surfaces.

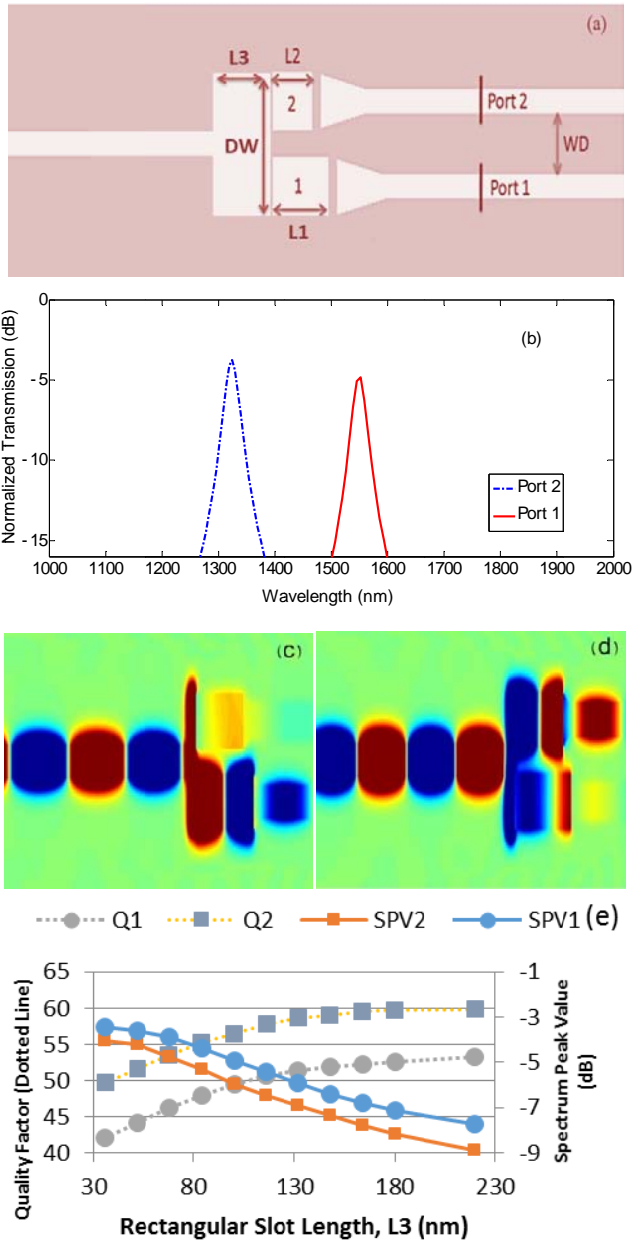


Fig. 2 (a) Schematic view of the proposed demultiplexer structure, (b) its transmission spectra with cavity lengths of  $L_1=628\text{nm}$ ,  $L_2=524\text{nm}$ , cavity widths of  $W_1=W_2=164\text{nm}$ , metallic gap size,  $G=16\text{nm}$ , waveguide width,  $d=100\text{nm}$ ,  $DW=416\text{nm}$ ,  $L_3=52\text{nm}$ . Magnetic field distributions for wavelengths of (c)  $1551\text{nm}$  and (d)  $1329\text{nm}$ , demonstrating the demultiplexing performance of the proposed device. (e) Quality factor (Q) and spectrum peak value (SPV) of both channels (Q1, Q2, SPV1, SPV2), versus rectangular slot length,  $L_3$ , waveguide width,  $d = 100\text{nm}$ ,  $L_1=628\text{nm}$ ,  $L_2=524\text{nm}$ , cavity widths of  $W_1=W_2=164\text{nm}$ , metallic gap size,  $G=16\text{nm}$ ,  $DW=416\text{nm}$

TABLE III  
SIMULATED SPECIFICATIONS OF THE RECTANGULAR DEMULTIPLEXER WITH  $D = 100\text{nm}$ ,  $L_1=628\text{nm}$ ,  $L_2=524\text{nm}$ , CAVITY WIDTHS OF  $W_1=W_2=164\text{nm}$ , METALLIC GAP SIZE,  $G=16\text{nm}$ ,  $DW=416\text{nm}$

$L_3(\text{nm})$	$Q_1, Q_2$	$SPV_1(\text{dB}), SPV_2(\text{dB})$	$\lambda_1(\text{nm}), \lambda_2(\text{nm})$
220	53,60	-7.7,-8.9	1319,1545
180	53,60	-7.1,-8.1	1319,1545
164	52,59	-6.8,-7.8	1319,1545
148	52,59	-6.4,-7.4	1319,1545
132	51,58	-5.9,-6.9	1319,1545
116	51,58	-5.4,-6.6	1319,1545
100	49,57	-4.9,-6.0	1319,1545
84	48,55	-4.4,-5.3	1319,1551
68	46,54	-3.9,-4.7	1324,1551
52	44,52	-3.6,-4.2	1329,1551
36	43,50	-3.3,-4.1	1349,1558

### REFERENCES

- [1] D. K. Gramotnev and S. I. Bozhevolnyi, "Plasmonics beyond the diffraction limit," *Nature Photon.* Vol. 4, pp. 83–91, 2010.
- [2] J. Zhang and L. Zhang, "Nanostructures for surface plasmons," *Advances in Opt. and Photon.* Vol. 4, pp. 157–321, 2012.
- [3] R. Zia, M. D. Selker, P. B. Catrysse, and M. L. Brongersma, "Geometries and materials for subwavelength surface plasmon modes," *J. Opt. Soc. Am. A*, Vol. 21, pp. 2442–2446, 2004.
- [4] H.S. Chu, I. Ahmed, W.B. Ewe, and E.P. Li, "Guiding light in different plasmonic nano-slot waveguides for nano-interconnect application," 2008 Asia-Pacific Symposium on Electromagnetic Compatibility & 19th International Zurich Symposium on Electromagnetic Compatibility, Singapore, pp. 590-593, May 2008.
- [5] Y. Guo, L. Yan, W. Pan, B. Luo, K. Wen, Z. Guo, H. Li, and X. Luo, "A plasmonic splitter based on slot cavity," *Opt. Express*, Vol. 19, pp. 13831-13838, 2011.
- [6] C.Y. Tai, S. H. Chang, and T. Chiu, "Design and Analysis of an Ultra-Compact and Ultra-Wideband Polarization Beam Splitter Based on Coupled Plasmonic Waveguide Arrays," *IEEE Photon. Technol. Lett.* Vol. 19, pp. 1448-1450, 2007.
- [7] J.H. Zhu, X.G. Huang, X. Mei, "Improved Models for Plasmonic Waveguide Splitters and Demultiplexers at the Telecommunication Wavelengths," *IEEE Trans. Nanotechnol.* Vol. 10, pp. 1166 - 1171, 2011.
- [8] S. Xiao, L. Liu, and M. Qiu, "Resonator narrow bandstop filters in a plasmon-polaritons metal," *Opt. Express*, Vol. 14, pp. 2932-2937, 2006.
- [9] A. Hosseini and Y. Massoud, "Nanoscale surface plasmon based resonator using rectangular geometry," *Appl. Phys. Lett.* Vol. 90, pp. 181102 (1-2), 2007.
- [10] A. Noulal, A. Akjouj, Y. Pennec, J.N. Gillet, and B. Djafari-Rouhani, "Modeling of two-dimensional nanoscale Y-bent plasmonic waveguides with cavities for demultiplexing of the telecommunication wavelengths," *New J. of Phys.* Vol. 11, pp. 103020 (1-19), 2009.
- [11] F. Hu and Z. Zhou, "Wavelength filtering and demultiplexing structure based on aperture-coupled plasmonic slot cavities," *J. Opt. Soc. Am. B*, Vol. 28, pp. 2518-2523, 2011.
- [12] H. Lu, X. M. Liu, L.R. Wang, D. Mao, and Y.K. Gong, "Nanoplasmonic triple-wavelength demultiplexers in two-dimensional metallic waveguides," *Appl. Phys. B*, Vol. 103, pp. 877–881, 2011.
- [13] K. Wen, L. Yan, W. Pan, B. Luo, Z. Guo, and Y. Gu, "Wavelength demultiplexing structure based on a plasmonic metal-insulator-metal waveguide," *J. Opt.* Vol. 14, 075001 (5pp), 2012.
- [14] C. Min and G. Veronis, "Absorption switches in metal-dielectric-metal plasmonic waveguides," *Opt. Express*, Vol. 17, pp. 10757-10766, 2009.
- [15] G.Y. Oh, D.G. Kim, and Y.W. Choi, "All-optical logic gate using waveguide-type SPR with Au/ZnO plasmon stack," 15th OptoElectronics and Communications Conference (OECC2010) Technical Digest, pp. 374-375, July 2010, Japan.
- [16] J. Tao, X.G. Huang, and J.H. Zhu, "A wavelength demultiplexing structure based on metal-dielectric-metal plasmonic nano-capillary resonators," *Opt. Express*, Vol. 18, pp. 11111-11116, 2010.

- [17] F. Hu, H. Yi, and Z. Zhou, "Wavelength demultiplexing structure based on arrayed plasmonic slot cavities," *Chin. Phys. Lett.*, Vol. 29, 104210, 2012.
- [18] W.L. Barnes, A. Dereux, and T.W. Ebbesen, "Surface plasmon subwavelength optics," *Nature*, Vol. 424, pp. 824-830, 2003.
- [19] S.A. Maier, *Plasmonics: Fundamentals and Applications*, Springer, 2007.
- [20] W. Cai and V. Shalaev, *Optical Metamaterials: Fundamentals and Applications*, Springer, 2010.
- [21] W.J. Tropf, M.E. Thomas, and T.J. Harris, Handbook of optics: Devices, Measurements, and Properties, Vol. II, Part 4: Optical And Physical Properties of Materials, Chapter 33: Properties of crystals and glasses, sponsored by the Optical Society of America, 1995.
- [22] Z. Han, V. Van, W.N. Herman, and P.T. Ho, "Aperture-coupled MIM plasmonic ring resonators with sub-diffraction modal volumes," *Opt. Express*, Vol. 17, pp. 12678-12684, 2009.
- [23] A. Setayesh, S.R. Mirnaziry, and M.S. Abrishamian, "Numerical investigation of a tunable band-pass plasmonic filter with a hollow-core ring resonator," *J. Opt.* Vol. 13, 035004 (7pp), 2011.